Rheol Acta 36:56–65 (1997)

ORIGINAL CONTRIBUTION

Erik A. Toorman

Modelling the thixotropic behaviour of dense cohesive sediment suspensions

Received: 22 May 1996
Accepted: 9 October 1996

Dr. E. A. Toorman (✉)
Hydraulics Laboratory
Civil Engineering Department
Katholieke Universiteit Leuven
De Croylaan 2
3001 Heverlee, Belgium
erik.toorman@bwk.kuleuven.ac.be

Abstract A dense cohesive sediment suspension, which contains primarily clay particles, is a thixotropic non-ideal Bingham fluid with a true yield stress. Its time-dependent rheological behaviour can be described by the structural kinetics theory in which the yield stress is taken as a measure for the structural parameter. This theory allows the construction of a more general equation of state, which is independent of the rate equation. The applicability of the model is demonstrated by examples of the prediction of constant structure curves and of transient behaviour. The thixotropy model is incorporated into a Navier-Stokes solver to stimulate the flow behaviour in a Couette viscometer.

Key words Thixotropy – structural kinetics theory – cohesive sediment suspension – numerical modelling

Notation

a Aggregation or recovery rate parameter
b Break-down rate parameter
c $=\mu_0-\mu_\infty$
k General rate parameter
r Radial coordinate
t Time
β Break-down to recovery rate ratio$=b/a$
$\dot{\gamma}$ Shear rate
η_∞ Dynamic viscosity for fully broken structure
λ Structural parameter$=\tau_y/\tau_0$
μ_0 Initial differential viscosity
μ_∞ Bingham viscosity
τ Shear stress
τ_0 Initial yield stress (fully recovered structure)
τ_B Bingham stress
τ_y Yield stress
τ_S Static yield stress
Ω Rotation speed
ω Angular velocity

Subscripts

e Equilibrium

Introduction

The study of the rheological behaviour of cohesive sediment suspensions, such as clay suspensions, is of practical importance in hydraulic engineering (dredging, hyperconcentrated flow, erosion resistance; e.g. Engelund and Wan, 1984, and Gularte et al., 1979), mining engineering (drilling muds; e.g. Nguyen and Boger, 1985), civil engineering (cement and grouts; e.g. Lapasin et al., 1983) and chemical engineering (ceramic materials; e.g. Moore, 1959). Since the early 1980s extensive studies have been carried out on the rheological behaviour of estuarine cohesive sediment suspensions. Important reviews have been presented by Williams (1984), Verreet and Berlamont (1989) and Williams and Williams (1989a, 1989b). This work is missing in the recent review by Coussot and Piau (1994).

Cohesive sediment suspensions can be characterized as non-ideal Bingham fluids, often with a true yield stress (Toorman, 1994). The present paper is a summary of an extensive theoretical study (Toorman, 1995) concerning the thixotropic behaviour (i.e. the mechanisms of structural recovery and shear thinning) of these suspensions, which is directly related to the flocculation of the clay particles and the break-up of these

flocs in shear flow (Michaels and Bolger, 1962). The mechanisms of these processes are discussed in further depth by Williams (1984) and van Leussen (1994), amongst others.

Moore (1959) introduced the structural kinetics theory as a model for describing the thixotropic behaviour of clay suspensions. Worrall and Tuliani (1964) extended this work by adding a yield stress term. It is remarkable that the application of this theory thus far seems to be restricted to the determination of the equilibrium flow curve and the transient behaviour under constant rate of deformation. In this paper it is shown that the same basic theory allows the construction of a more general equation of state, which is independent on the rate equation and which can be applied to any flow history.

Before continuing, it is important to make a general remark on rheometrical data for flocculated suspensions. In this work the model is tested on available published data as they are presented, without making corrections for possible wall effects, as is often done. However, the quality or relevance of many data sets should be seriously questioned, because the majority of the rheometrical devices work with too small gaps or produce shear layers which are too narrow for valid shear flow generation in fine-grained granular suspensions. The likely occurrence of wall slip or depletion in the shear layer, even for vane spindles, could explain the often measured decrease of the shear stress with increasing rotation speed (or deformation rate) at low deformation rates. Hence, considering the fact that the chance for slip in a concentric cylinder viscometer is very high for small rotation speeds, one cannot be sure that the measured values and flow curve features at low shear rates are correct (Toorman, 1994). Therefore, one has to be very careful when experimental data are interpreted. The problem of wall depletion is too often underestimated (Barnes, 1995).

Thixotropy model

Structural kinetics

To quantify the time dependent rheological behaviour of flocculated suspensions, a non-dimensional structural parameter λ is introduced. This parameter is a measure of the degree of structure in the suspension, having a value in the range 0 (fully broken) to 1 (fully structured). In analogy with chemical reaction kinetics, a rate equation, which expresses that the structural state is the net result of structural break-down and recovery, is defined (Moore, 1959). It is assumed that the rate of break-down depends on the deformation rate $\dot{\gamma}$ and on the fraction of links existing at any instant and therefore is assumed to be written as $-b\dot{\gamma}\lambda^n$. Similarly, the rate of build-up is assumed to be proportional to the fraction of links remaining to be formed, which is assumed to equal $\lambda_0-\lambda$, to a certain power m. The maximum value of the structural parameter λ_0 is commonly assumed to equal 1. In the following, the exponents m and n are both assumed to be equal to 1, leading to the original first-order rate equation, proposed by Moore (1959):

$$\frac{d\lambda}{dt} = a(\lambda_0 - \lambda) - b\dot{\gamma}\lambda \tag{1}$$

where the aggregation or recovery rate parameter a and the break-down parameter b are empirical parameters.

At equilibrium, the rate of break-down equals the rate of recovery. The locus of points in the $\tau - \dot{\gamma}$ plane, which fulfil this condition, form the equilibrium flow curve (EFC). Since at equilibrium $d\lambda/dt=0$, the equilibrium value of the structural parameter λ_e can be obtained from Eq. (1), i.e.:

$$\lambda_e = \frac{a\lambda_0}{1+b\dot{\gamma}} = \frac{\lambda_0}{1+\beta\dot{\gamma}} \tag{2}$$

where $\beta=b/a$. λ_e is thus a function of the shear rate. Hence, Eq. (1) can be rewritten in the form:

$$\frac{d\lambda}{dt} = -(a+b\dot{\gamma})(\lambda - \lambda_e) \tag{3}$$

The yield stress, which is a measure of the internal strength of the flocculated structure, seems to be the most appropriate measurable property which can be related to structure (Billington, 1960; Cheng, 1986). Therefore, following the proposal of Billington (1960), the structural parameter λ is defined here as:

$$\lambda = \frac{\tau_y}{\tau_0} \tag{4}$$

where τ_0 is the yield stress of the EFC, i.e. $\tau_0=\tau_y\,(\lambda=1)$.

Equation of state

In analogy with the model proposed by Moore (1959), Worrall and Tuliani (1964) added a structural term to the Bingham model. However, this does not account for the essential fact that the yield stress should be a function of the structural parameter, according to Eq. (4). Therefore, the general equation of state for a thixotropic yield stress fluid is written as:

$$\tau = \tau_y(\lambda) + \mu(\dot{\gamma},\lambda)\dot{\gamma} = \lambda\tau_0 + (\eta_\infty(\dot{\gamma}) + c\lambda)\dot{\gamma} \tag{5}$$

where η_∞ is the dynamic viscosity of the suspension at $\lambda=0$ (i.e. completely broken-down structure).

The concept of a time-dependent yield stress has been considered by several researchers. Slibar and Paslay (1964) however assumed a constant Bingham

viscosity and an exponential memory function. Tiu and Boger (1974) simply multiplied the two terms in the Hershel-Bulkley model with a structural parameter. Nguyen and Boger (1985) only analyzed data of the time variation at constant rate of deformation.

The equilibrium flow curve found by Worrall and Tuliani (1964), expressed in terms of the parameters of the EFC, can be written in a rate equation independent form as:

$$\tau_e = \lambda_0\tau_0 + (\mu_\infty + c\lambda_e)\dot{\gamma} \tag{6}$$

where μ_∞ is the Bingham viscosity and τ_0 (in the original equation) has been replaced by $\lambda_0\tau_0$, which does not make any difference since $\lambda_0 = 1$. The equilibrium points are given by expressing Eq. (5) at a specified λ_e. Equating this to Eq. (6), one finds the following relationship:

$$(\lambda_0 - \lambda_e(\dot{\gamma}))\tau_0 + (\mu_\infty - \eta_\infty(\dot{\gamma}))\dot{\gamma} = 0 \tag{7}$$

Substitution of Eq. (7) into Eq. (5), eliminating η_∞, yields:

$$\tau = (\lambda_0 + \lambda - \lambda_e(\dot{\gamma}))\tau_0 + (\mu_\infty + c\lambda)\dot{\gamma} \tag{8}$$

Equation (8) represents a new rheological equation for a thixotropic yield stress fluid expressed in terms of the EFC parameters. Notice that this formulation does not put any constraints on the rate equation, i.e. it is valid for every type of rate equation!

For the specific first-order rate equation, Eq. (3), the following equilibrium flow curve is found:

$$\tau = \lambda_0\tau_0 + \mu_\infty\dot{\gamma} + \frac{c\lambda_0\dot{\gamma}}{1+\beta\dot{\gamma}} \tag{9}$$

Analysis of many rheometrical data on clay and (estuarine) mud suspensions strongly suggests that this gives the best representation of its equilibrium flow curve (Toorman, 1994). From Eqs. (2) and (7) the relationship for the non-structured viscosity can be found:

$$\eta_\infty(\dot{\gamma}) = \mu_\infty + \frac{\lambda_0\beta\tau_0}{1+\beta\dot{\gamma}} = \mu_\infty + \lambda_e\beta\tau_0 \tag{10}$$

Substitution of Eq. (10) into Eq. (5) yields:

$$\tau = \lambda\tau_0 + (\mu_\infty + c\lambda + \beta\tau_0\lambda_e)\dot{\gamma} \tag{11}$$

It should be realized that in nearly every point of the EF curve $\tau_y(\lambda_e) \neq \tau_0$ and $\mu(\dot{\gamma}_e) \neq \mu_\infty$. The values of τ_y and η_∞ depend on the structural parameter and thus vary along the EF curve. It is indeed observed that the value of the Bingham parameters decreases due to structural break-down (decreasing λ). The values of the parameters of the EF curve however are independent.

Calibration

The proposed complete thixotropy model requires the determination of five empirical parameters. Four of them, i.e. τ_0, μ_∞, c and β, are found through least squares fitting of the EF curve. The rate equation parameters can be obtained from transient data. When the deformation rate is constant, the rate equation can be integrated analytically. For instance, integration of the n-th order form of Eq. (3), i.e. $\mathrm{d}\lambda/\mathrm{d}t = -k(\lambda - \lambda_e)^n$, at constant shear rate gives:

$$\begin{aligned}&((\tau_y - \tau_{y,e})/\tau_0)^{-(n-1)}\\ &\quad = (n-1)kt + ((\tau_{y,i} - \tau_{y,e})/\tau_0)^{-(n-1)} \quad (n > 1)\end{aligned} \tag{12}$$

$$\ln(\tau_y - \tau_{y,e}) = \ln(\tau_{y,i} - \tau_{y,e}) - kt \quad (n = 1)$$

where $k = a + b\dot{\gamma} = a(1 + \beta\dot{\gamma})$. Several published data indeed show this linear behaviour (e.g. Tiu and Boger, 1974; Nguyen and Boger, 1985). This allows the determination of the recovery rate parameter a and the order n of the rate equation.

Constant structure curves

The locus of points in the $\tau - \dot{\gamma}$ plane which correspond to the same value of the structural parameter λ form the constant structure curve (CSC). When the EF curve is known and can be described by Eq. (9), a simple procedure allows the computation of the CS curves. For each data point of the EF curve the value of the structural parameter value is obtained from Eq. (2). Substitution of this value into Eq. (11) gives the CS curve. Notice that the construction of the CS curves does not require the knowledge of the recovery and break-down rate parameters (a and b) individually, only their ratio β.

In concentric cylinder viscometry experimental data are obtained in terms of torque versus rotation speed. For non-Newtonian fluids the true shear rate is not only a function of geometrical parameters of the device, but also from the a priori unknown rheological parameters of the tested material. Several methods (sometimes referred to as "shear rate correction methods") have been derived to compute the true shear rate at the wall for fully sheared and partially sheared (or plug) flow (Yang and Krieger, 1978; Toorman, 1994). Hence, one of these shear rate calculation methods should be applied to obtain the actual EF curve. The rheological parameters can be found with a curve fitting method (e.g. least-squares).

This procedure has been applied to two data sets of clay suspensions (Cheng and Evans, 1965; and Joye and Poehlein, 1971). A comparison of measured and predicted CS curves for these cases is presented in

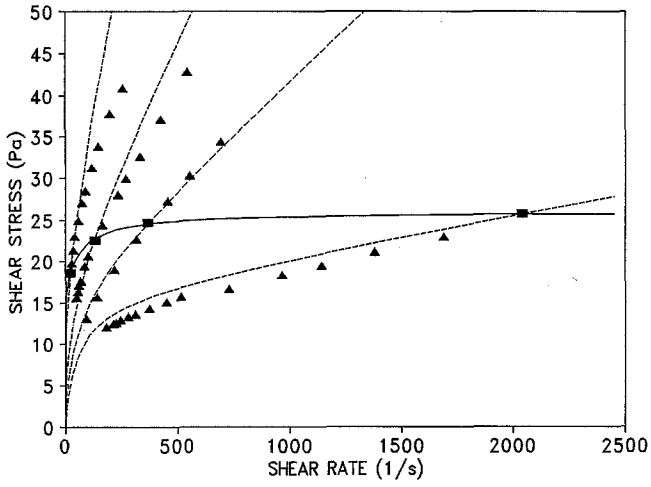

Fig. 1 Equilibrium flow and constant structure curves for a 6.5% bentonite suspensions. Symbols=experimental data (Cheng and Evans, 1965); full line=equilibrium flow curve; dashed lines=constant structure curves according to Eq. (8). Model parameters: $\mu_\infty = 0.0$ Pa·s, $\mu_0 = 0.1512$ Pa·s, $\tau_0 = 15.59$ Pa, $\tau_B = 26.17$ Pa

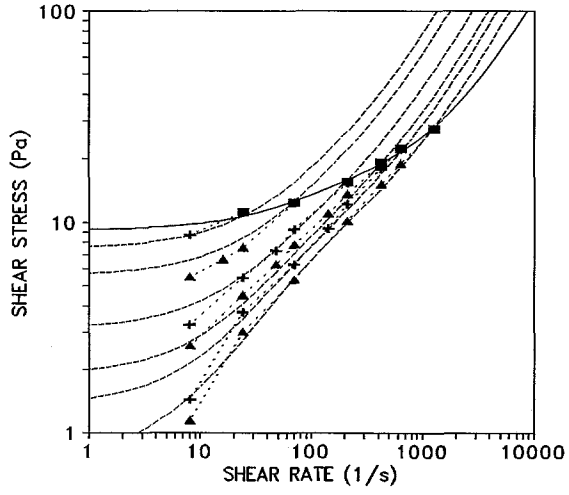

Fig. 2 Equilibrium and constant structure curves for a hectorite suspension. Symbols (connected by dotted lines)=experimental data (Joye and Poehlein, 1971); full line=equilibrium flow curve; dashed lines=constant structure curves according to Eq. (8). Model parameters: $\tau_0 = 9.2$ Pa, $\tau_B = 16.2$ Pa, $\mu_\infty = 0.0098$ Pa·s, $\mu_0 = 0.074$ Pa·s

Figs. 1 and 2. The experimental points of the CS curves have been obtained with the shear-rate step-change method (Cheng, 1986). The agreement between model and experiment is surprisingly good. There are several potential causes for the deviations:

a) Experimental errors, particularly wall slip;
b) The Moore model may be too crude (or the rate equation is not first-order);
c) The shear rate calculation method of Cheng and Evans (1965), which also allows the determination of the shear rate of CS curve data, may introduce too large truncation or differentiation approximation errors;
d) Cheng and Evans' method does not account for the possibility that the material may not always be sheared over the total gap width.
e) As Joye and Poehlein (1971) do not mention any shear rate calculation, it is likely that they assume a linear velocity profile over the 1-mm-wide gap. This may be a theoretically valid approximation under specific circumstances (narrow gap, fully sheared flow without wall slip), which, however, are unlikely to be achievable in reality, particularly at low shear rates.

For further validation, transient flow tests should be considered.

Numerical implementation

The rate equation can be solved to yield the structural parameter at each time step, using a numerical discretization scheme. This can very easily be incorporated into any numerical code, requiring only the storage into a vector of the values of the structural parameter for each node of the computational mesh, which are replaced by the new value at each time step. Shear rate intensities are obtained from the flow field computation (e.g. a Navier-Stokes solver).

When there is no advection, the spatial derivatives of λ are absent and differentiation of Eq. (3) with a Cranck-Nicholson scheme yields:

$$\frac{\lambda_t - \lambda_{t-\Delta t}}{\Delta t} = -\frac{(a + b\dot{\gamma}_t)(\lambda_t - \lambda_e) + (a + b\dot{\gamma}_{t+\Delta t})(\lambda_{t+\Delta t} - \lambda_e)}{2} \quad (13)$$

from which one obtains the simple algebraic expression:

$$\lambda_t = \frac{\lambda_{t-\Delta t}\left[\frac{2}{\Delta t} - a - b\dot{\gamma}_{t-\Delta t}\right] + 2a}{\frac{2}{\Delta t} + a + b\dot{\gamma}_t} \quad (14)$$

where Δt is the time step of the numerical scheme.

A practical problem often will be the lack of knowledge of the initial structural conditions in each node. When initially the sample is at rest after sufficiently long storage the structure may be considered fully recovered, i.e. $\lambda(t = 0) = \lambda_0 = 1$. This can be best justified when the rheological parameters are determined from samples taken at time zero of the test. Indeed, in that case the reference value τ_0 is the highest yield stress value to be expected (unless the material is allowed to recover even more in certain areas of the domain which are left undisturbed).

It should be noted that the present model generates a non-zero initial stress in a fluid at rest, which value is determined by the initial value of the structural parameter, i.e. $\tau(\dot{\gamma}=0)=\lambda\tau_0$. In reality, a dense cohesive sediment suspension at rest will consolidate (effective stresses will develop) and it transforms into a soft soil with visco-elastic properties. Under an external shear force, the material will first deform elastically, until the stress within the material exceeds the yield value. This rapid initial visco-elastic stress build-up is missing in the present model. Therefore, the use of the model is restricted to visco-plastic flow behaviour only (i.e. when the yield stress is exceeded), e.g. for use with a Navier-Stokes solver. It is for this purpose that the model has been developed. The elastic contribution is present in the model by Coussot et al. (1993), who proposes a Bingham model where the yield stress is described by a Maxwell-like viscoelasticity combined with a structural kinetics equation.

Secondary structure

Many investigations on clay and mud suspensions reveal an initial yield stress which is significantly higher than the Bingham stress and the corresponding flow curve shows a minimum. Cheng (1986) distinguishes this high *static* yield (τ_S) stress from the lower *dynamic* yield stress (τ_D), which is the extrapolated value of the EF curve (Fig. 3). For some materials the static yield stress can be attributed to a known secondary structure, which breaks down rapidly and recovers very slowly or only under specific ambient conditions. An explanation for the occurrence of a static yield stress in some clay suspension (e.g. Englund and Wan (1984) found a stress minimum in the flow curve of concentrated bentonite suspensions, but not for kaolinite) does not seem to be known.

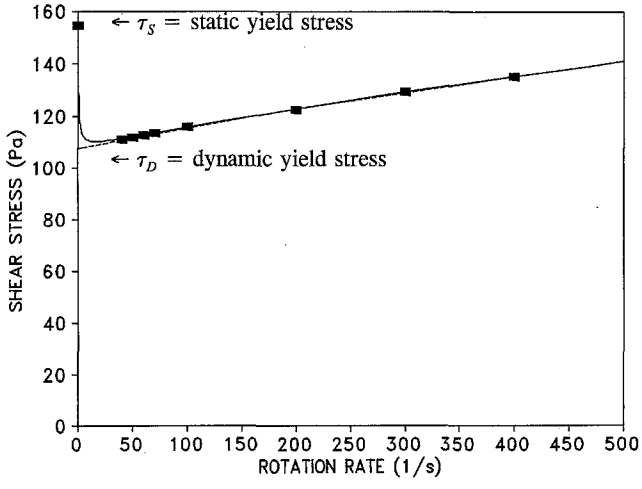

Fig. 3 Static and dynamic yield stress for the equilibrium flow curve of a 4% aqueous bentonite suspension. Symbols=experimental data (*Coussot et al.*, 1993); dotted line=curve fit, excluding static yield stress τ_S (Eq. 9); solid line=including τ_S (Eq. 15). Parameter values: τ_S=154.2 Pa, τ_D=105 Pa, $\tau_{B=}$110 Pa, μ_∞=0.064 Pa·s, μ_0=0.2 Pa·s, β_S=2 s

Although it is still a subject of discussion whether a flow curve minimum is physically possible, several observations seem impossible to be explained otherwise. A flow curve with a minimum leads to unstable flow phenomena. For instance, with a simple experimental test and a theoretical model (in which thixotropy is not taken into account) Engelund and Wan (1984) showed that the existence of a flow curve minimum provides the only explanation for observed clogging behaviour and subsequent water level oscillations in hyperconcentrated river flow. This was verified by comparison of tests on suspensions with bentonite (flow curve minimum, oscillating flow) and kaolinite (no minimum, stable flow).

A simple way to include the secondary structure in the equation of state is to add a new term to the equation of state with a second structural parameter λ_S:

$$\tau=\lambda_S(\tau_S-\tau_D)+\lambda\tau_D+(\mu_\infty+c\lambda+\beta\tau_D\lambda_e)\dot{\lambda} \quad (15)$$

The parameter λ_S can be computed from a second rate equation of the same form as for the primary structure. Notice that flow curve data, such as presented in Fig. 3, can be fitted with different sets of model parameters for Eq. (15). Additional experimental data are required to determine the only correct values. The correctness of this equation, both physically and mathematically, and of the determination of its parameters requires further investigation.

The simulation of start-up flow data, presented below, required the inclusion of a secondary structural contribution, in order to predict correctly the overshoot peaks. Equation (15) proved to be useful for this purpose.

However, the occurrence of a stress minimum in flow curves obtained with conventional viscometers should be reviewed in the light of possible biassing of the measurements due to wall slip.

Simulation of transient behaviour

Stress decay/recovery at constant shear rate

Nearly all published simulations of transient behaviour of thixotropic fluids are restricted to relaxation under a constant deformation rate, which often can be described by a linear relationship given by Eq. (12) (e.g. Tiu and Boger, 1974; Nguyen and Boger, 1985).

For any point of the EF curve, the sudden change from one rotation speed to a higher or lower one results

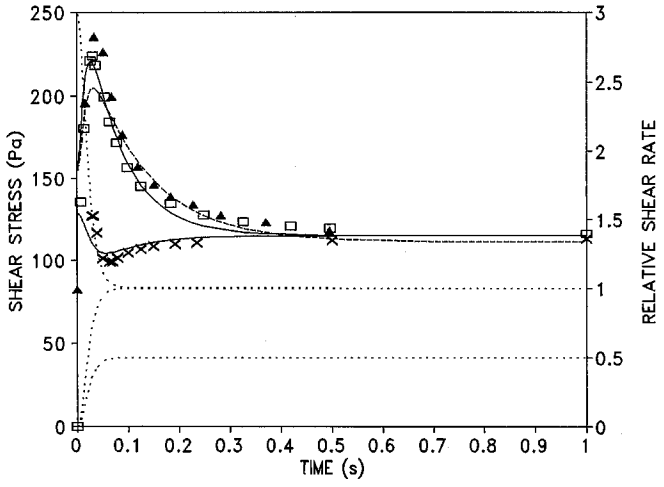

Fig. 4 Comparison between start-up flow of a 4% bentonite-water mixture for $\dot{\gamma}=0 \rightarrow 100\ s^{-1}$ (□=experiment; upper full line=simulation), $\dot{\gamma}=0 \rightarrow 50\ s^{-1}$ (▲=experiment; dashed line=simulation) and $\dot{\gamma}=300 \rightarrow 100\ s^{-1}$ (×=experiment; lower full line=simulation). Dotted line=assumed shear rate evolution relative to $100\ s^{-1}$ (T= 0.013 s). Experimental data from Coussot et al. (1993). Parameter values (the same for all simulations) as in Fig. 3 and $b=0.09$, $b_S=0.02$

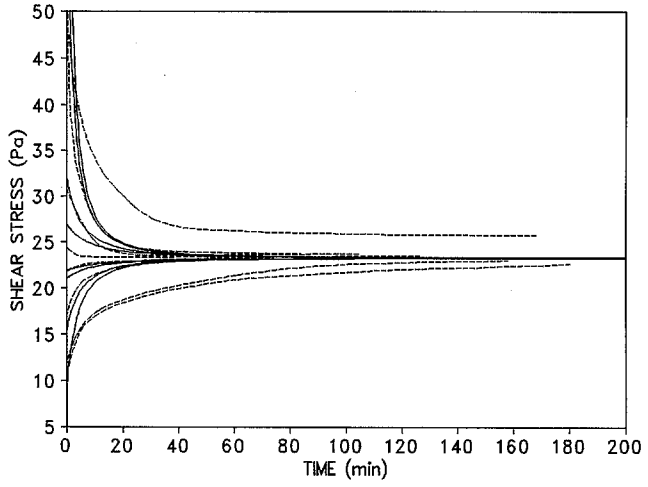

Fig. 5 Comparison between measured (dashed lines) and computed (full lines) stress relaxation at a constant shear rate of $48.6\ s^{-1}$ for different initial values of the structural parameter in a 14% aqueous bentonite suspension. Experimental data from Mylius and Reher (1972). Best correspondence for a rate equation of order $n=1.5$

in a stress over- or undershoot respectively because the material requires time to adapt to the new shear distribution. The maximum stress is thus reached after a finite time. The simulation of the data presented by Coussot et al. (1993), assuming a sudden change in shear rate, predicts the stress peak to occur nearly immediately (also in the simulation by Coussot et al. themselves), unlike the experimental data. Hence, the relatively large delay in the occurrence of the stress maximum cannot be explained by the material response as described by the present or Coussot's model. It can only be simulated if it is assumed that the shear rate change takes a certain time (Fig. 4), which may correspond to a certain response time of the devive to a change in rotation speed (e.g. inertia of the rotating body or the gearing system). Therefore, in the simulation of Coussot's data, a change in shear rate from $\dot{\gamma}_0$ to $\dot{\gamma}_1$ is imposed as $\dot{\gamma}(t) = \dot{\gamma}_0 + (\dot{\gamma}_1 - \dot{\gamma}_0)(1 - \exp(-t/T))^3$, where T is a reference time scale for the transition period.

The result of the model simulation is presented in Fig. 4. The break-down parameter values have been calibrated with the experimental data. The other parameter values are obtained from the EF curve. It is assumed that the material initially is at equilibrium. The occurrence of a higher stress peak for a smaller step change in the experiment is unexpected, unless the initial structure was stronger than assumed.

Also one stress relaxation experiment by Mylius and Reher (1972) has been simulated (Fig. 5). Here again, the flow curve (Fig. 6) shows a stress minimum. The flow curve has been obtained in a narrow gap concentric cylinder viscometer in which it is expected that

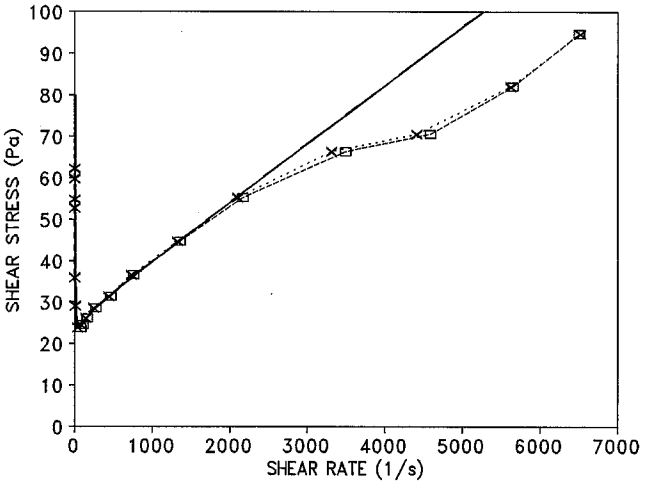

Fig. 6 Equilibrium flow curve of the 14% aqueous bentonite suspension, corresponding to Fig. 5. ×=experimental data (Mylius and Reher, 1972); □=shear rate corrected data using Yang and Krieger's (1978) method; full line=used curve fit including secondary structure modification

wall depletion is very important. Therefore the flow curve may be completely biassed as wall depletion implies the measurement of much smaller shear stresses than obtained if the material was sheared within itself (Barnes, 1985). Nevertheless, accounting for the apparent secondary structure gives reasonable agreement with measurements. Not all of the experimental curves follow a perfect exponential decay or reach the same equilibrium value as in the model prediction (Fig. 5). This illustrates the difficulty of reproducing the same initial structural conditions in the experiment, which is another possible cause of the deviations between experiment

and computation. Notice that the difference between the experimental flow curve data points and those obtained with Yang and Krieger's (1978) shear rate calculation method do not differ much (Fig. 6), which indicates that a linear approximation of the velocity profile in a narrow gap configuration at high rotation speeds can be acceptable.

Hysteresis

All sorts of numerical experiments can be carried out by computing the stress evolution for a certain imposed shear rate history. In Fig. 7 the simulation of a cyclic shear rate history, is shown giving the typical hysteresis loops. This ultimately results in an equilibrium loop, which shape is determined by the rate of change of the shear rate and which intersects the EF curve at two points (at least if the maximum applied shear rate is large enough) as expected (Cheng and Evans, 1965). Comparison of these model results with experimental data by Gabrysh et al. (1962, 1963) shows that the predicted hysteresis behaviour is very realistic. Often a small overshoot peak at low shear rate occurs in the published data, which again suggests the presence of a secondary structure. Indeed, addition of a secondary structure term, as in Eq. (15), can produce such a peak (Fig. 7 a).

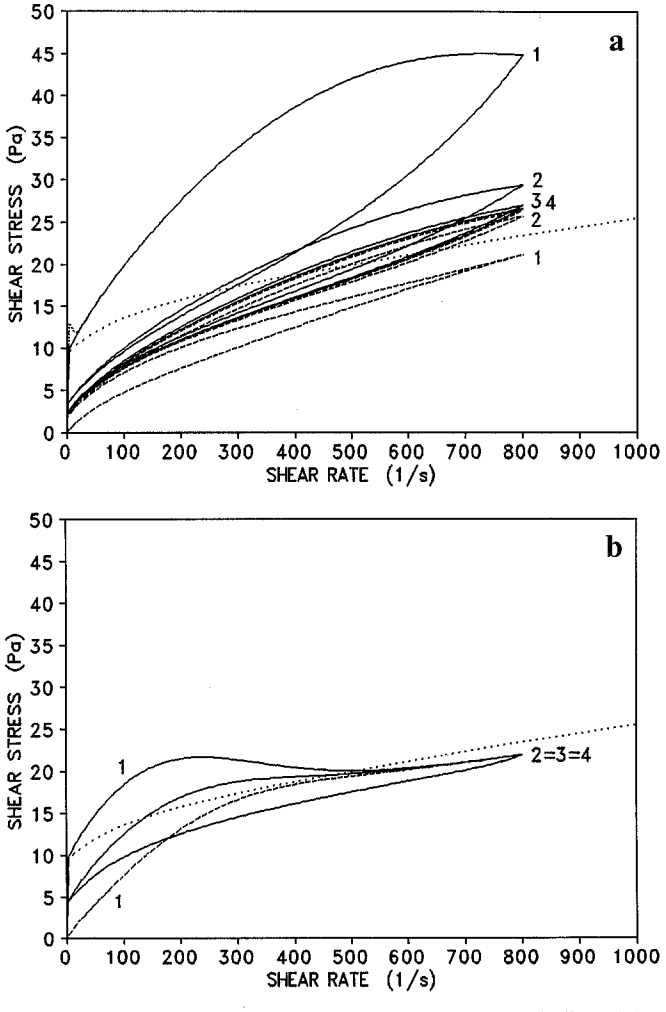

Fig. 7 Flow history of four subsequent cycles (order indicated by number) of steadily increasing and subsequent decreasing of the shear rate at a rate of a) 40 and b) 4 s^{-1}/s. Rheological parameters as in Fig. 2 and a=0.01 s^{-1}. Full line: $\lambda(t=0)=1$; dashed line: $\lambda(t=0)=0$; centred line=effect of added fictitious secondary structure (τ_S=20 Pa, β_S=2 s, b_S=0.5); dotted line=equilibrium flow curve

Simulation of Couette flow

The velocity profile over the gap of a concentric cylinder viscometer can be computed as the solution of the angular (or tangential) momentum conservation equation:

$$\rho\frac{\partial u}{\partial t}=\rho r\frac{\partial \omega}{\partial t}=\frac{1}{r^2}\frac{\partial}{\partial r}(r^2\tau)=\frac{\partial \tau}{\partial r}+2\frac{\tau}{r}$$
$$=\frac{1}{r^2}\frac{\partial}{\partial r}\left[r^3\mu\frac{\partial \omega}{\partial r}\right]=3\mu\frac{\partial \omega}{\partial r}+r\frac{\partial}{\partial r}\left[\mu\frac{\partial \omega}{\partial r}\right] \quad (16)$$

where: u=tangential velocity (θ-component of the velocity vector), $\omega=u/r$=angular velocity and r=radial coordinate. This equation can be written in many different ways, depending on how the derivatives are further developed. Some of these forms lead to unstable schemes. Equation (16) is discretized with a first-order implicit finite difference scheme as follows:

$$\rho r_i\frac{\omega_i-\omega_{i,0}}{\Delta t}=3\mu_i\frac{\omega_{i+1}-\omega_{i-1}}{2\Delta r}$$
$$+\frac{r_i}{\Delta r}\left[\frac{\mu_{i+1}+\mu_i}{2}\frac{\omega_{i+1}-\omega_i}{\Delta r}\right.$$
$$\left.-\frac{\mu_i+\mu_{i-1}}{2}\frac{\omega_i-\omega_{i-1}}{\Delta r}\right] \quad (17)$$

This equation is solved together with Eqs. (8) and (14). This has to be done iteratively because they are non-linear since the viscosity is a function of the shear rate, which is described by a central difference discretization of the velocity gradient. The boundary conditions are: $\omega_{bob}=\Omega(t)$ and $\omega_{cup}=0$ rad/s.

In the Figs. 8–10 the results of the numerical solution of the flow field in a controlled rotation speed concentric cylinder viscometer for a fictitious rotation speed history are shown. The bob radius is 10 mm and the cup radius is 15 mm. Over the gap 100 nodes have been taken. The time step Δt = 1 s. The rheological parameters of the hectorite suspension from Fig. 2 have been used.

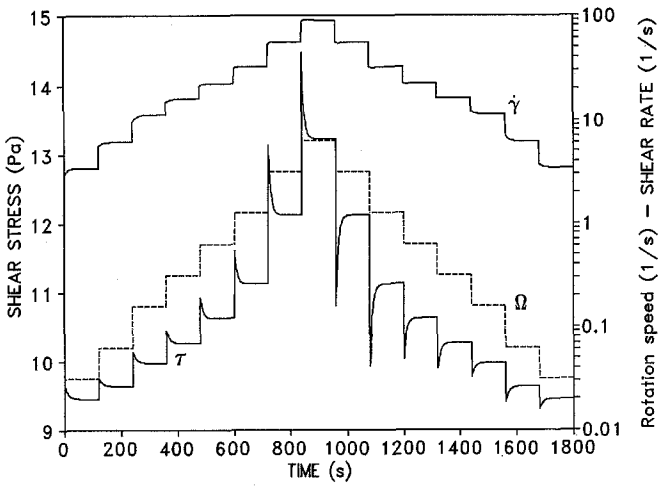

Fig. 8 Simulated shear stress and shear rate evolution at the bob wall for a classical stepwise controlled rate concentric viscometer test (with rotation speed change spread over a small, finite period; rheological parameters as in Fig. 2)

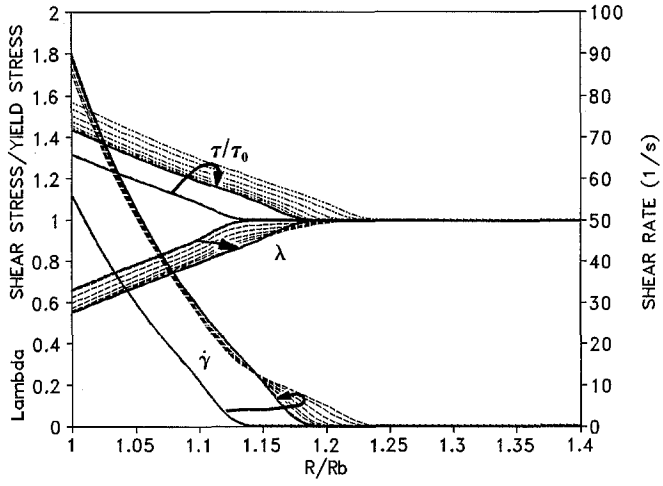

Fig. 10 Computed shear rate, shear stress and structural parameter profile evolution (arrows) for a step change from $\Omega = 30$ to 60 rpm (parameters as in Fig. 2)

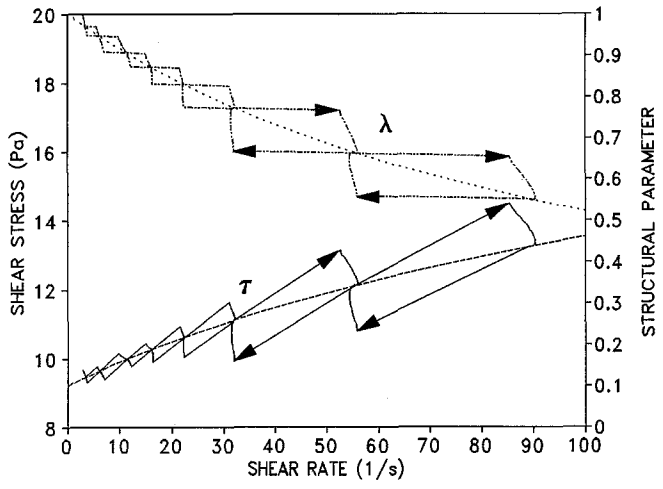

Fig. 9 Flow and structural history corresponding with Fig. 8. Full line $= \tau(t)$; dashed line $= \tau_e$ (EFC); centred line $= \lambda(t)$; dotted line $= \lambda_e$ (locus of equilibrium structure); arrow indicates time progression

When a sudden step-change in rotation speed as it occurring in one time step is imposed as boundary condition, there is often oscillation of the solution due to the overshoot peak (depending on the value of the time step). When the change of the rotation speed is allowed to vary rapidly, but continuously over a small, finite period, the stress peaks reduce (this could physically represent the response time of the device, as mentioned above). In the simulation the delay of the velocity change is obtained by applying relaxation to the bob surface velocity boundary condition.

Figure 8 shows the time evolution of the imposed rotation speed and the computed shear rate and shear stress correspondingly. The results clearly show that the shear rate follows a transient behaviour and does not follow the rotation speed immediately. In Fig. 9 the history of the shear stress and the structural parameter in function of the shear rate is shown. At each step change of the rotation speed the stress suddenly changes while the structure remains the same (horizontal arrow). Subsequently, both stress and structure slowly return to the equilibrium condition corresponding to the actual rotation speed.

Figure 10 shows computed profiles of shear rate, shear stress and structure at different time steps between the initial and the final equilibrium state during the change from a certain rotation speed to a higher one. The material is only partially sheared over the wide gap. The computed shear rate and stress profiles show nicely how the yield surface, where $\dot{\gamma} = 0$, moves further away from the centre (from $r_y/r_b \approx 1.14$ to 1.19) with increasing the rotation speed and even shows an overshoot during the transient period. The shear rate profiles clearly show how thin the actual sheared layer is (only about 2 mm in this case). The solutions deviate from the expected solution when the radius approaches the (time-dependent) yield radius. This is because of the problem of the infinite vicosity beyond the yield radius, which cannot be dealt with numerically. In practice, the maximum viscosity must be delimited. This corresponds to a so-called bi-viscosity approach, often applied for yield stress fluids (e.g. Beverly and Tanner, 1992; Toorman, 1992). This is obtained by limiting the minimum shear rate to 10^{-4} s^{-1}.

Conclusions

The rheological behaviour of dense cohesive sediment suspensions is time-dependent due to changes in the flocculated structure as a result of shear rate variations. It is a thixotropic fluid. The degree of structure is quantified with the introduction of a structural parameter. The yield stress seems to be the most convenient measurable property to represent the structural parameter.

Application of the structural kinetics theory, as proposed by Moore (1959), allows the construction of the equation of state for the description of any flow history of a cohesive sediment suspension. The basic model introduces five parameters, of which four can be determined from the equilibrium flow curve. The fifth parameter can be obtained from a recovery experiment or from other transient data.

Several data sets suggest the existence of a static yield stress, higher than the equilibrium or dynamic yield stress. This could indicate the presence of a double structure (i.e. possible two types of interparticle bonds exist). The secondary structure, corresponding to the static condition, probably extends throughout the sample and is possibly related to a certain state as obtained during consolidation. Its recovery seems to be much slower than that of the primary structure. The model has been extended to account for this phenomenon by introducing a second structural parameter. However, the interpretation of equilibrium flow curves with a minimum should be reviewed in the light of the likely occurrence of wall depletion.

Two data sets for clay suspensions from the literature, presenting the equilibrium flow curve and constant structure curves, are well described by the new model. Next, the model has been validated with transient data. Unfortunately, the data sets found in the literature are suspected to be biassed by the occurrence of wall slip. Nevertheless, two sets of published data for a step-change in shear rate experiment on bentonite suspensions could be simulated reasonably well. The fact that these data sets can be simulated satisfactorily indicates that the proposed model may be a very useful tool for the mathematical description of the thixotropic behaviour of clay and related material suspensions.

The occurrence of stress overshoots after a step-change in deformation rate are generally overestimated and occur nearly immediately according to the model. In reality a delay of the stress peak is observed and the peak period is wider. This can be completely explained and simulated by considering a continuous, rather than a sudden change in the deformation rate. This seems to be more realistic because of inertia effects in rheometrical devices.

Results from tests of the model (e.g. the hysteresis test) provide an explanation for the underprediction of the rheological parameters, which have been obtained through conventional flow curve measurements (see e.g. the mud pumping simulation by Toorman, 1992). Indeed, in the latter case one obtains values which correspond rather close to equilibrium values. Due to the combined effects of slow break-down and recovery these values may never be reached in reality. The hysteresis test shows that the equilibrium hysteresis has two intersections with the EF curve. Hence the actual viscosities can be much higher than those obtained from the EF curve.

Other data sets suggest that β may be dependent on the shear rate or that in many cases the rate equation should be of higher order (Toorman, 1995). This requires further investigation. The importance of wall slip effects should be studied in more detail. The elimination of wall slip for dense flocculating fine-sediment suspensions is a problem because the effective shear layer thickness in conventional viscometers is often too thin (Toorman, 1994).

Acknowledgments The author's position of post-doctoral researcher has been granted by the Belgian National Fund for Scientific Research. This work has been carried out in connection with research undertaken as part of the MAST-2 G8M Costal Morphology programme, partly funded by the Commission of European Communities, Directorate General for Science, Research and Development, under contract MAS2-CT92-0027.

References

Barnes HA (1995) A review of the slip (wall depletion) of polymer solutions, emulsions and particle suspensions in viscometers: its cause, character and cure. J Non-Newtonian Fluid Mechanics 56:221–251

Beverly CR, Tanner RI (1992) Numerical analysis of three-dimensional Bingham plastic flow. J Non-Newt Fl Mech 42:85–115

Billington EW (1960) Some measurements of the time dependence of the viscosity of thixotropic fluids. Proc Phys Soc 75:40–50

Cheng DC-H, Evans F (1965) Phenomenological characterization of the rheological behaviour of inelastic reversible thixotropic and antithixotropic fluids. Brit J Appl Phys 16:1599–1617

Cheng DC-H (1985) Yield stress: a time-dependent property and how to measure it. Rheol Acta 25:542–554

Coussot P, Leonov AI, Piau JM (1993) Rheology of concentrated dispersed systems in a low molecular weight matrix. J Non-Newt Fl Mech 46:179–217

Coussot P, Piau JM (1994) On the behavior of fine mud suspensions. Rheol Acta 33:175–184

Engelund F, Wan Z (1984) Instability of hyperconcentrated flow. J Hydr Eng 110:219–233

Gabrysh AF, Eyring H, Cutler I (1962) Rheological factors for attapulgite suspended in water. J Am Ceramics Soc 45(7):334–343

Gabrysh WF, Eyring H, Lin-Sen P, Gabrysh AF (1963) Rheological factors for bentonite suspensions. J Am Ceramics Soc 46(11):3523–3529

Gularte RC, Kelly WE, Nacci VA (1979) Rheological methods for predicting cohesive erosion. Proc Ann Conf Marine Technological Soc 251–258

Joye DD, Poehlein GW (1971) Characteristics of thixotropic behaviour. Trans Soc Rheol 15:51–61

Lapasin R, Papo A, Rajgelj S (1983) The phenomenological description of the thixotropic behavior of fresh cement pastes. Rheol Acta 22:410–416

Michaels AS, Bolger JC (1962) The plastic flow behaviour of flocculated kaolin suspensions. I&EC Fundamentals 1(3):153–162

Moore F (1959) The rheology of ceramic slips and bodies. Trans Brit Ceramic Soc 58:470–494

Mylius E, Reher EO (1972) Modelluntersuchungen zur Charakterisierung thixotroper Medien und ihre Anwendung für verfahrenstechnische Prozeßberechnungen. Plaste und Kautschuk 19(6):410–431

Nguyen QD, Boger DV (1985) Thixotropic behaviour of concentrated bauxite residue suspensions. Rheol Acta 24:427–437

Slibar A, Paslay PR (1964) On the analytical description of the flow of thixotropic materials. In: Reiner M, Abir D (eds) Second-order effects in elasticity, plasticity and fluid dynamics. Pergamon Press, Oxford 314–330

Tiu C, Boger DV (1974) Complete characterization of time-dependent food products. J Texture Studies 5:329–338

Toorman EA (1992) Modelling of fluid mud flow and consolidation. PhD thesis, Civil Eng Dept, Katholieke Universiteit Leuven, 219 pp

Toorman EA (1994) An analytical solution for the velocity and shear rate distribution of non-ideal Bingham fluids in a concentric cylinder viscometer. Rheol Acta 33:193–202

Toorman EA (1995) The thixotropic behaviour of dense cohesive sediment suspensions. Report HYD149, Hydraulics Laboratory, K.U. Leuven, 69 pp

van Leussen W (1994) Estuarine macroflocs and their role in fine-grained sediment transport. PhD thesis, University of Utrecht, 448 pp

Verreet G, Berlamont J (1989) Rheology and non-Newtonian behavior of sea and estuarine mud. In: Cheremisinoff NP (ed) Rheology and Non-Newtonian Flows. Encyclopedia of Fluid Mechanics 7:135–149

Williams DJA (1984) Rheology of cohesive suspensions. In: Mehta AJ (ed) Estuarine cohesive sediment dynamics. Lecture Notes on Coastal and Estuarine Studies 14:110–125

Williams DJA, Williams PR (1989a). Rheology of concentrated cohesive sediment. In: Mehta AJ, Hayter EJ (eds) High concentration cohesive sediment transport. J Coastal Research, Special Issue No. 5:165–173

Williams PR, Williams DJA (1989b). Rheometry for concentrated cohesive suspensions. In: Mehta AJ, Hayter EJ (eds) High concentration cohesive sediment transport. J Coastal Research, Special Issue No. 5:151–164

Worrall WE, Tuliani S (1964) Viscosity changes during the ageing of clay-water suspensions. Trans Brit Ceramic Soc 63:167–185

Yang TMT, Krieger IM (1978) Comparison of methods for calculating shear rates in coaxial viscometers. J Rheol 22:413–421